

Parametric Modeling and Control of a Long-Range Actuator Using Magnetic Servo Levitation

Hector Martin Gutierrez and Paul I. Ro

Abstract— A mechatronic device based on magnetic servo levitation (MSL) is proposed for long range and wide bandwidth actuation. The force capability of this type of actuator can be significantly larger than a linear motor or voice-coil actuator of similar dimensions. A novel parametric model of the electromagneto-mechanical coupled system has been developed to describe its behavior over a large range of motion and frequency, as opposed to more conventional attractive force small-perturbation models. It also provides a convenient way of devising a feedback linearizing control scheme that eliminates the need for high biasing currents present in most magnetic bearing systems. This paper presents a feedback-linearized controller coupled with a Kalman filter as a first approach to solve the tracking problem for such an actuator. Good tracking performance have been found both in simulation and experiments.

Index Terms— Feedback linearization, magnetic servo levitation, parametric modeling.

I. INTRODUCTION

MAGNETICALLY driven devices represent a promising but very challenging alternative to actuate positioning systems where both long range and fast response (wide bandwidth) are required. Magnetic servo levitation (MSL) [1], [4] has been proposed as an alternative that allows ranges up to 1 mm while being free of friction and backlash problems accompanied by conventional mechanical actuators. It can also exert significantly larger force than linear motors or voice-coil actuators of similar dimensions [1].

While MSL could provide an adequate bandwidth within a range of motion twenty times larger than a piezoelectric-based actuator, there are a number of fundamental issues that make implementation difficult.

A long-range MSL-based system is open loop unstable and highly nonlinear, and its dynamics can not be properly represented by simplified models. It is important to emphasize the need of both a highly accurate model and a robust control law if high positioning accuracy is to be achieved.

II. ELECTROMAGNET DESIGN

The electromagnets used in the device presented in this paper have an “E”-shaped geometry (Fig. 1) with the coil

Manuscript received November 24, 1996; revised April 15, 1998. This work was supported in part by the Office of Naval Research under Contract N00014-94-1-0235.

The authors are with the Precision Engineering Center, North Carolina State University, Raleigh, NC 27695 USA.

Publisher Item Identifier S 0018-9464(98)05837-3.

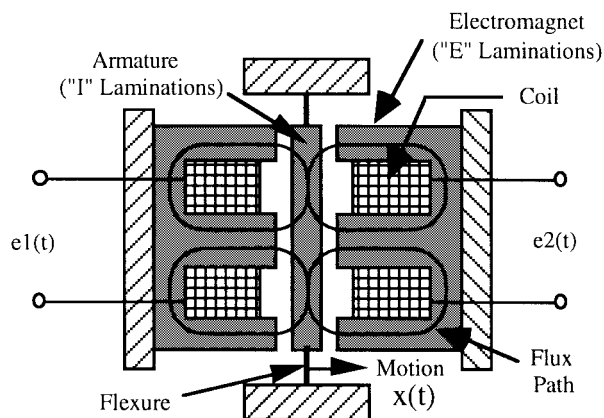


Fig. 1. Electromagnet concept.

mounted on the middle leg of the “E,” both core and armature consisting of stacks of iron-silicon alloy laminations.

The most relevant design equations [14] are average flux F

$$\Phi = \frac{Ni}{\frac{l}{\mu_r \mu_0 A} + \frac{2g}{\mu_0 A}}$$

and magnetic force F given by

$$F = \left(\frac{Ni\mu_r}{l + 2g\mu_r} \right)^2 \mu_0 A$$

where N is number of turns, i the coil current, l the length of the flux path, g nominal gap, A the pole area, μ_r relative permeability of the laminations, and μ_0 permeability of air. These equations were used to size the electromagnets and determine overall dimensions of the system. Two pairs of small electromagnets were preferred over one large pair to facilitate heat dissipation and to provide a path for a feedback sensor to pass through.

Another important design aspect was to determine operating regimes that would allow the actuator to drive within the linear region of the magnetic material. Static BH curves for the alloy under consideration show linear behavior for magnetic field density B up to 1.2 Tesla. Beyond 1.6 Tesla, an increase on field intensity H do not provide a significant increase on B and therefore magnetic force starts to saturate. The maximum coil current in a given magnet at any given time should therefore be a function of the corresponding air gap.

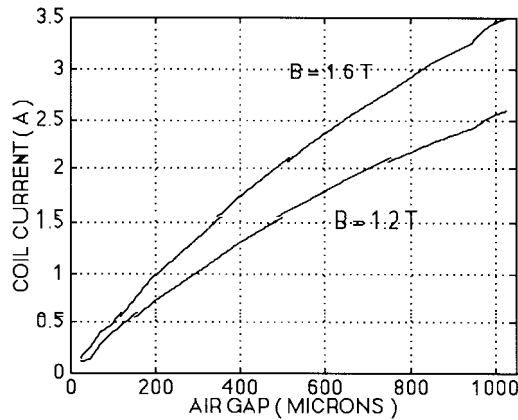


Fig. 2. Actuator operating regions.

To establish operating regions, several finite-element field simulations were run in order to find which coil current would produce a magnetic induction of 1.2 or 1.6 Tesla for a given gap at critical points within the core profile; results are shown on Fig. 2. This procedure is not very straight forward since some points in the core tend to saturate even when most of the core is holding relatively small values of B ; a tradeoff between saturation and core utilization had to be established by the designer.

From this procedure, operating regions can be sketched. At any given time, the coil current command for a given gap should be (if possible) under the 1.2 T curve. Any current command beyond the 1.6 T line is considered unacceptable since it increases power dissipation without improving available magnetic force. The region in between the two curves is acceptable but discouraged.

This operating region map is used jointly with computer simulations to determine whether a given control command (coil current) is acceptable or not. The finite-element solutions also allowed the verification that opposing electromagnets are magnetically decoupled when currents are in the desired operating region.

III. MECHANICAL DESIGN

An electromagnetic actuator for tool motion correction based on MSL is depicted in Fig. 3. This type of actuator can be used as an active tool holder for machining operations such as diamond turning [7]. The design had to avoid unnecessary mass (that could reduce the natural frequency of the system) without sacrificing structural stiffness. Flexures were chosen stiff enough to keep the natural frequency of the system above the desired bandwidth but compliant enough to achieve the desired range of motion. The nominal air gap is adjustable, allowing for a tradeoff of bandwidth for range if necessary.

Position feedback can be obtained from several different types of sensors depending on range, accuracy, and cost specifications. Most experiments presented here were carried out using an infrared optical probe, but a capacitance gauge or a laser interferometer could be equally well suited. Experiments conducted on a test fixture with a single pair of flexures

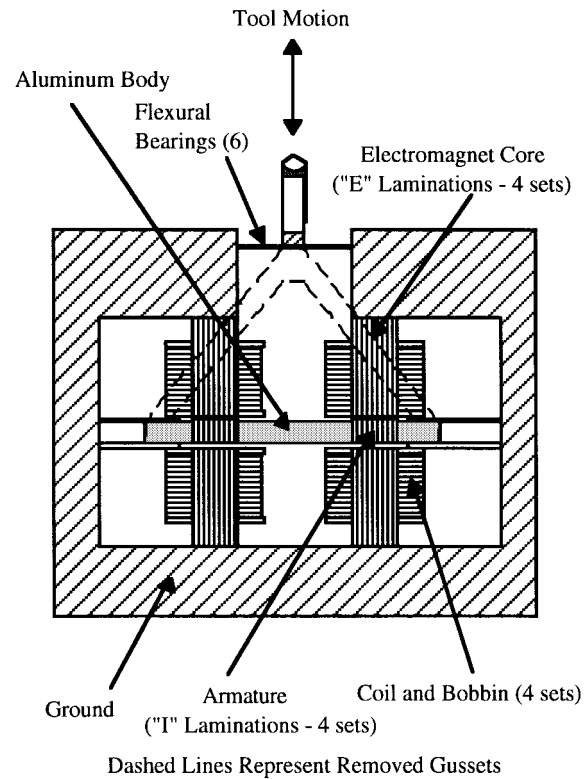


Fig. 3. Actuator schematic.

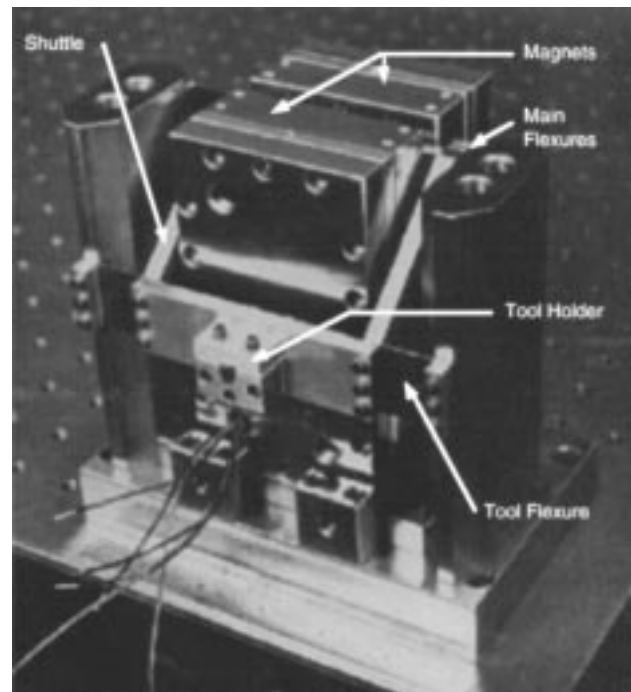


Fig. 4. Actuator prototype.

showed a second and third dynamic modes within 100 Hz of the first resonant peak that added complex oscillatory modes to the system. To avoid this, an additional set of flexures was included to move such modes 1000 Hz above the first resonance; this was verified both by finite element calculations and experimentally. A picture of the electromagnetic actuator is shown in Fig. 4.

IV. MATHEMATICAL MODELING OF ELECTRO-MAGNETO-MECHANICAL SYSTEMS

Modeling an electromagnetic actuator for long-range high-precision applications requires taking into account several aspects of the system that prevent the use of simplified models, which in general share two basic assumptions: uniform magnetic field density within the core material and linear magnetic core operation (constant magnetic permeability). Although for short-range low-bandwidth applications [6], [9], linear versions of such models seem to work reasonably well, a long range actuator, where displacement can not be described as small perturbations of a nominal trajectory requires a model that is accurate over a wide range of displacement and frequencies.

An electromagnetic actuator is a coupled system where motion equations are to be solved simultaneously with electromagnetic and circuit equations. Current literature emphasizes the use of finite element methods to solve the electromagnetic field equations through the magnetic circuit [10]–[12]. Strong coupling models are based on incorporating the motion equations into a finite element model of the field equations [11]. In parametrized coupled models [10], the field equations are solved off-line by finite elements to determine magnetic force and flux as static functions of current and position; the solutions are then used to solve the circuit and motion equations by interpolating force and flux values according to measured position and current. Although FEM-based models have the appeal of being based on first principles of physics, they all involve a number of approximations and are sensitive to both structural and parametric uncertainties.

The authors have explored the use of parametrized coupled models of the long-range fast-tool servo depicted on Figs. 3 and 4. Measured I/O sequences were compared to model based simulations, obtained by interpolating force and flux values from discrete solutions generated through FEM calculations and using them to integrate circuit and motion equations. It has been established that for the intended application, these models are not accurate enough.

V. PARAMETRIC MODEL OF MAGNETIC SERVO LEVITATION

Electromechanical systems driven by magnetic forces, such as magnetic bearings [9] or micro-positioning stages [6] typically have a very small range of motion (on the order of a few microns) and small bandwidth (on the order of a few Hertz). For this reason, simple mathematical models of the magnetic force seem to work reasonably well, namely

$$F_{\text{mag}} = K \frac{i^2}{g^2}$$

where i is coil current, g is air gap, and K some constant to be determined. Furthermore, some of these systems operate at high bias current levels, thus allowing the use of Jacobian (small signal) linearization. In the case of a magnetically levitated actuator, none of these assumptions hold true. This prompts for the development of a different modeling strategy. A mathematical model can be formulated in such a way that

input nonlinearities are separable and additive

$$a_1 \frac{d^2x}{dt^2} + a_2 \frac{dx}{dt} + a_3x = F_{\text{mag}2} - F_{\text{mag}1} \quad (1)$$

where x is displacement, a_i are unknown parameters, and each magnetic force F_{mag} can be described as some polynomial of coil current (i) and the corresponding air gap. For instance

$$F_{\text{mag}2} = \sum_{j=1}^n \left(K_{1j} \frac{i_2}{(x_0 - x)^{0.5j}} + K_{2j} \frac{i_2^2}{(x_0 - x)^{0.5j}} \right). \quad (2)$$

In these equations, x is measured from the equilibrium position, x_0 is the nominal air gap, and K_{ij} are parameters to be determined. The problem is to find the unknown coefficients in (1) and (2) such that experimental I/O sequences can be fitted in a minimum mean-square error sense. In order to use linear parametric techniques to find optimal fits for these parameters, each rational term in (2) can be considered a separate input to the system in such a way that (1) can be written as

$$\frac{d}{dt} \begin{bmatrix} x \\ \frac{dx}{dt} \end{bmatrix} = \begin{bmatrix} 0 & 1 \\ -\frac{a_3}{a_1} & -\frac{a_2}{a_1} \end{bmatrix} \begin{bmatrix} x \\ \frac{dx}{dt} \end{bmatrix} + \begin{bmatrix} 0 & 0 & \cdots & 0 \\ K_{11} & K_{21} & \cdots & K_{4n} \end{bmatrix} \begin{bmatrix} u_1 \\ u_2 \\ \cdots \\ u_{4n} \end{bmatrix}. \quad (3)$$

The techniques used to estimate the parameters involved are called prediction error methods [5], [13], and are based on the minimization of a cost function which is the sum of the squared prediction errors. The general case of the parametric estimation problem for linear multiple-input single-output systems can be formulated as the estimation of the coefficients of polynomials A , B , C , D , E , and F in

$$A(q)y(t) = \frac{B_1(q)}{F_1(q)} u_1(t - mk_1) + \cdots + \frac{B_n(q)}{F_n(q)} u_n(t - mk_n) + \frac{C(q)}{D(q)} e(t) \quad (4)$$

where $y(t)$ is the current output prediction, $e(t)$ is an unmodeled disturbance, and q is the delay operator defined as $q^{-1}f(t) = f(t - T)$, T being the sampling rate. The auto-regressive moving average model with exogenous input (ARMAX model) is a special case of (4) with $F_1(q) = \cdots = F_n(q) = D(q) = 1$. The coefficients of the other polynomials can be grouped as a vector of unknown parameters (q), namely

$$\theta = [\alpha_1, \cdots, a_{n_a}, b_1^1, \cdots, b_{n_b1}^1, \cdots, b_1^{nu}, \cdots, b_{n_bnu}^{nu}, \cdots, c_1, \cdots, c_{n_c}]^T \quad (5)$$

where nu is the number of inputs. The Bayesian prediction error is defined as

$$\varepsilon(t|\theta) = y(t) - \hat{y}(t|\theta). \quad (6)$$

The ARMAX one-step predictor can be shown to be [13]

$$\hat{y}(t|\theta) = B_{o_1}(q)u_1(t) + \cdots + B_{o_{nu}}(q)u_{nu}(t) + [1 - A(q)]y(t) + [C(q) - 1]\varepsilon(t|\theta) \quad (7)$$

where the polynomials B_{oj} include the delay terms on (4). Defining the one-step ahead regression vector

$$\phi(t|\theta) = [-y(t-1), \dots, -y(t-n_a), u_1(t-1), \dots, u_1(t-n_{b1}), \dots, u_{nu}(t-1), \dots, u_{nu}(t-n_{bnu}), \dots, \varepsilon(t-l|\theta), \dots, \varepsilon(t-n_c|\theta)]^T. \quad (8)$$

The ARMAX regression model can now be written as

$$\hat{y}(t|\theta) = \theta^T \phi(t|\theta) = \phi^T(t|\theta)\theta. \quad (9)$$

The estimation problem is aimed to minimize the prediction error cost function

$$J_N(\theta) = \frac{1}{2N} \sum_{t=1}^N \varepsilon^2(t, \theta). \quad (10)$$

Defining $E(\theta) = [e(1|q), \dots, e(N|q)]^T$ and the matrix $O(\theta)$ such that $o_{jt}(q) = \partial \varepsilon(t|\theta) / \partial \theta_j$, the gradient g of J_N can be expressed as

$$g(\theta) = \frac{\partial J(\theta)}{\partial \theta} = \frac{1}{N} O(\theta)E(\theta) \quad (11)$$

and similarly, the Hessian matrix H of J_N is given by

$$H = \frac{\partial^2 J}{\partial \theta^2} = \frac{1}{N} O(\theta)O(\theta)^T + \frac{1}{N} \frac{\partial O(\theta)}{\partial \theta} E(\theta). \quad (12)$$

This defines the Gauss-Newton algorithm for updating the parameter vector, namely, for a step size s

$$\theta_{i+1} = \theta_i - sH^{-1}g(\theta_i). \quad (13)$$

Approximating H as the left term at the right side of (12), the algorithm becomes

$$\theta_{i+1} = \theta_i - s(OO^T)^{-1}O(\theta_i)E(\theta_i). \quad (14)$$

Using (6) and (9), the vector $E(\theta)$ is defined as a function of both I/O measurements and the vector of unknown parameters. Then (11)–(13) define the algorithm that updates q until the minimum value (or a local minimum) of J_N is reached. Previous knowledge or “reasonable guesses” of the system’s parameters (e.g., effective mass, estimated spring stiffness) significantly improves the speed of convergence and minimizes the chance of hitting local minima since they provide initial estimates to the algorithm. Notice that this procedure converges to a unique set of parameters and therefore models the system as time-invariant.

Parameters of the magnetically-levitated servo system model (3) were estimated using the Gauss-Newton algorithm (11)–(13) by first converting (3) to the discrete domain and then expressing the system’s equations as the ARMAX model derived from the general form (4). Model parameters were determined from exciting the system with band-limited noise; model response was then analyzed with different excitation signals. A sample of results (actual output and model predicted output) is shown in Fig. 5. More details and experimental results can be found in [7].

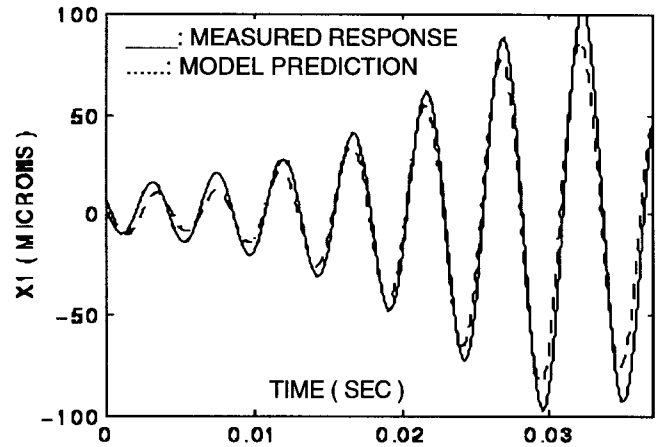


Fig. 5. Response to a swept sine wave.

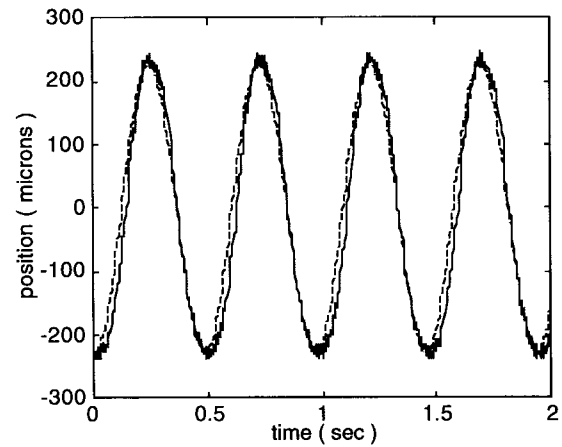


Fig. 6. Response to sine wave command (2 Hz).

VI. CONTROLLER DESIGN FOR MAGNETIC LEVITATION BASED ON FEEDBACK LINEARIZATION

The existence of extensive literature in linear controller design prompted for an implementation that could make use of such techniques, provided they could be implemented without affecting performance by incurring on unnecessary approximations. The model structure (2), (3), is particularly well-suited for feedback linearization as described in [2] and [8]. This is an approach to nonlinear controller design that differs entirely from conventional linearization (i.e., small signal analysis) in the sense that linearization is achieved by exact state transformations and feedback rather than by a linear approximation of the dynamics. The system is not constrained to operate around some nominal trajectory nor must the input signal be “small” compared to the input bias level. Applications that use Jacobian linearization (such as many magnetic bearing controllers) require biasing currents approximately ten times larger than the control current in order to achieve reasonable performance.

The mathematical foundations of feedback linearization can be found at [2] and [8]. The MSL fast-tool servo can be feedback-linearized by the following input coordinate trans-

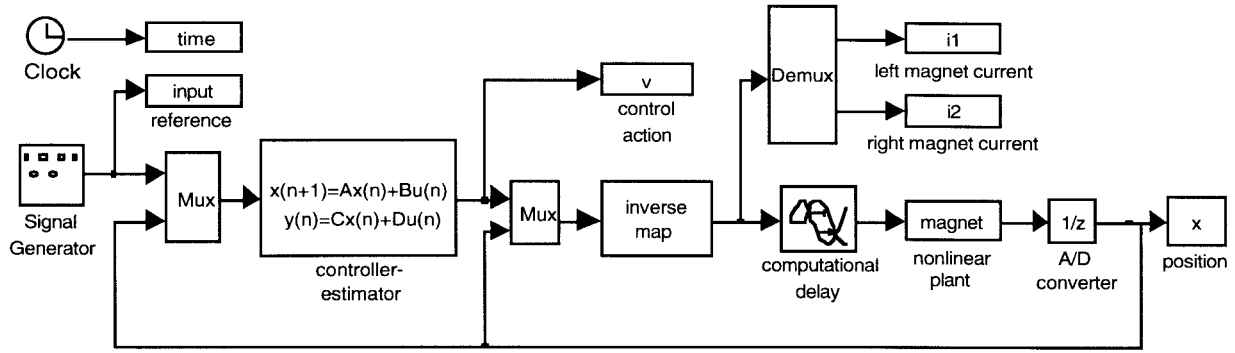


Fig. 7. Closed-loop magnetically levitated system with LQR controller-estimator.

formation

$$\begin{aligned} \frac{dX}{dt} &= AX + f(X, i_1, i_2) = AX + f(X, U) \\ \frac{dX}{dt} &= AX + \begin{bmatrix} 0 & 0 \\ 1 & 1 \end{bmatrix} \begin{bmatrix} v_1 \\ v_2 \end{bmatrix} \end{aligned} \quad (15)$$

where $f(X, U)$ represents the input nonlinearity described by (2). The problem becomes a standard linear controller design problem, and the performance is limited by the range of the input space $\langle v_1, v_2 \rangle$ over which the inverse maps $i = f^{-1}(x, v)$ are well defined. To further clarify this point, consider again (1) and (2). Terms containing input currents can be factored as follows

$$\begin{aligned} a_1 \frac{d^2x}{dt^2} + a_2 \frac{dx}{dt} + a_3x \\ = K_1(x)i_1 + K_2(x)i_1^2 + K_3(x)i_2 + K_4(x)i_2^2. \end{aligned} \quad (16)$$

The following input coordinate transformation becomes obviously convenient

$$\begin{aligned} v_1 &= K_3(x)i_1 + K_4(x)i_1^2 \\ v_2 &= K_1(x)i_2 + K_2(x)i_2^2 \end{aligned} \quad (17)$$

which renders the system linear as in (15). This transformation is valid subject to the existence of the corresponding inverse maps, i.e.,

$$\begin{aligned} i_1 &= \sqrt{\frac{1}{K_4(x)} \left(v_1 + \frac{K_3^2(x)}{4K_4(x)} \right)} - \frac{K_3(x)}{2K_4(x)} \\ i_2 &= \sqrt{\frac{1}{K_2(x)} \left(v_2 + \frac{K_1^2(x)}{4K_2(x)} \right)} - \frac{K_1(x)}{2K_2(x)}. \end{aligned} \quad (18)$$

Once the system is linearized, controller design can be carried out based on a linear quadratic regulator, using a reduced-order discrete Kalman filter to estimate the non-measurable states. The closed loop system is depicted on Fig. 7. Controller-estimator matrices computed off-line were implemented on a 486-PC equipped with a A/D D/A board; the closed loop rate used was 2.5 kHz. Experimental results are shown in Figs. 6, 8, and 9 (in all plots: command signal: dashed line, measured response: solid line).

The open loop system has poor tracking capabilities, as can be seen in a singular value plot in the frequency domain. For this reason, the integral of the tracking error was added as an

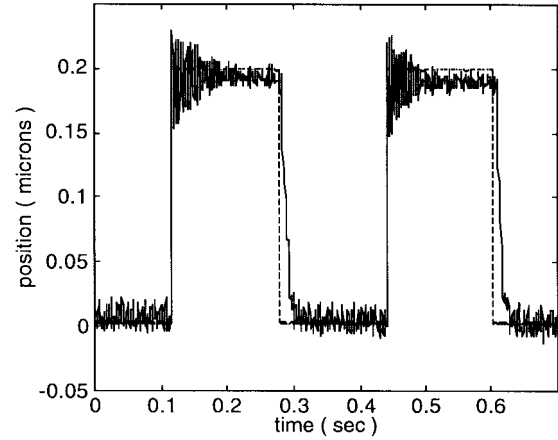


Fig. 8. Step response (3 Hz).

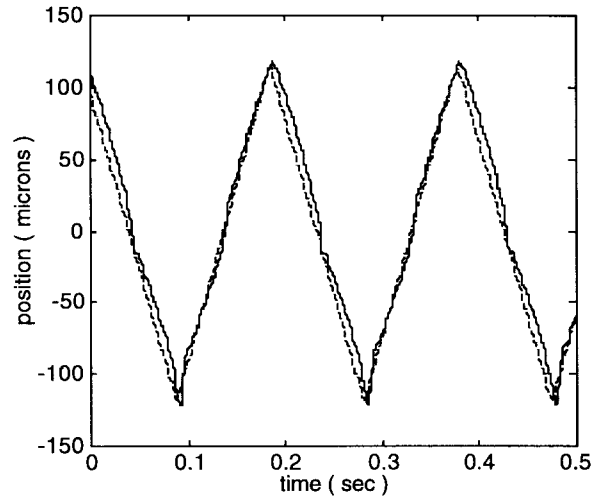


Fig. 9. Response to ramp command (5 Hz).

additional state to take advantage of the regulatory capabilities of the linear quadratic regulator (LQR) design [3]. Figs. 6, 8, and 9 illustrate the tracking capabilities of the feedback linearization scheme with augmented LQR compensator.

One significant achievement of this approach is the ability to track both long and short stroke ranges (Figs. 6 and 8). Tracking performance, however, degrades when either range or frequency bounds are exceeded (Fig. 10).

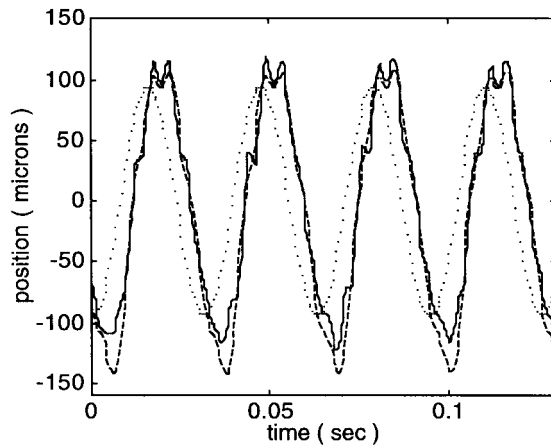


Fig. 10. Tracking performance degradation (command: dotted, measured: dashed, simulated: solid).

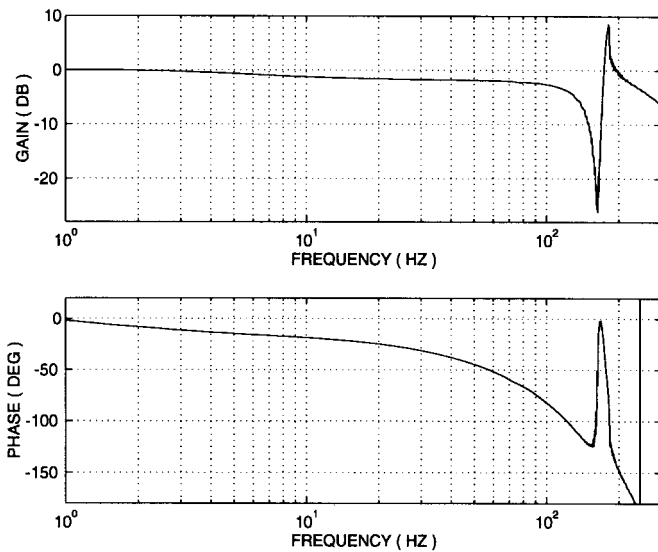


Fig. 11. Closed-loop frequency response.

To examine model error and closed loop rate as possible causes of performance limitation, input coil currents were recorded while operating the system in closed loop. Current coil data was later sent through a simulation network corresponding to (1) and (2) in order to evaluate the ability of the model to reproduce the behavior of the actual plant. Results are shown in Fig. 10, showing good agreement between simulated and measured response. Hardware used for these tests limited the closed loop rate to 2.5 kHz; the difference in response between actual plant and linearized system is expected to decrease as closed loop rate increases, provided the model is valid at the given operating conditions.

While these results illustrate both the feasibility of achieving long-range tracking and the adequacy of the modeling technique here presented, there are a number of factors that degrade overall performance and need to be investigated. Sensitivity to parameter uncertainties, unmodeled dynamics, and computational time delay seem to have a significant impact on tracking performance. Domain boundaries imposed by the inverse maps (18), sensor noise, and amplifier bandwidth

(frequency band over which the power amplifiers behave as ideal current sources) may also be affecting overall closed loop performance.

Experimental frequency response of the closed loop system is shown in Fig. 11, illustrating the range at which good tracking (0 dB gain) can be achieved with the current setup.

VII. CONCLUSIONS

MSL represents a promising alternative to long range electromagnetic actuation while keeping an adequate bandwidth.

A novel mathematical model of magnetic levitation has been presented and used for controller design. The model has been experimentally tested both by simulating actual I/O data and by closed loop tests. An adequate model is essential to control a long-range electromagnetic actuator since there is a highly nonlinear map between error signal and control action (coil currents).

The proposed scheme has shown good tracking capabilities, although within a limited range and bandwidth. Feedback linearization is affected by time varying parameters and other unmodeled dynamic effects; robust nonlinear controller design techniques therefore represent an interesting path for future research.

ACKNOWLEDGMENT

The authors gratefully acknowledge D. Trumper from the Massachusetts Institute of Technology for his help on electromagnet design at an early stage of this project.

REFERENCES

- [1] M. Tsuda and T. Higuchi, "Design and control of magnetic servo levitation," *Rep. Inst. Ind. Sci.*, Univ. Tokyo, vol. 37, no. 2, pp. 137–205, Mar. 1992.
- [2] J. J. Slotine and W. Li, *Applied Nonlinear Control*. Englewood Cliffs, NJ: Prentice-Hall, 1987.
- [3] G. F. Franklin and J. D. Powell, *Digital Control of Dynamic Systems*. Reading, MA: Addison-Wesley, 1980.
- [4] T. Higuchi, M. Tsuda, and Y. Nakamura, "Design of magnetic servo levitation for robot mechanisms," in *Proc. 20th Int. Symp. Ind. Robots*, 1989, pp. 136–144.
- [5] L. Ljung, *System Identification: Theory for the User*. Englewood Cliffs, NJ: Prentice-Hall, 1987.
- [6] D. L. Trumper, S. J. Ludwick, and M. L. Holmes, "Design and control of a 6-DOF magnetic/fluidic motion control stage," in *Proc. ASME-Int. Mech. Eng. Congr. Exhibition*, San Francisco, CA, vol. 57, no. 1, pp. 511–518, 1995.
- [7] H. M. Gutierrez, B. A. Stancil, and P. I. Ro, "Design and modeling of a magnetically levitated fast-tool servo system for precision turning," in *Proc. ASME-Int. Mech. Eng. Congr. Exhibition*, San Francisco, CA, vol. 57, no. 1, pp. 491–497, 1995.
- [8] A. Isidori, *Nonlinear Control Systems*. London, U.K.: Springer-Verlag, 1995.
- [9] K. Youcef-Toumi, S. Reddy, and I. Vithiananthan, "Digital time delay controller for active magnetic bearings," presented at *2nd Int. Symp. Magn. Bearings*, Tokyo, Japan, 1990, pp. 15–22.
- [10] Z. Ren and A. Razek, "Modeling of dynamic behaviors of electromagneto-mechanical coupled systems," in *Proc. 2nd Int. Conf. Comput. Electromagn.*, U.K., 1994, pp. 20–23.
- [11] G. Bedrosian, "New method for coupling finite-element field solutions with external circuits and kinematics," *IEEE Trans. Magn.*, vol. 29, pp. 1664–1668, Mar. 1993.
- [12] F. Piriou and A. Razek, "Simulation of electromagnetic systems by coupling of magnetic and electric equations," *Math. Comput. Simul.*, vol. 31, pp. 189–194, 1989.
- [13] P. Van den Bosch and A. Van der Klauw, *Modeling Identification and Simulation of Dynamical Systems*. Boca Raton, FL: CRC Press, 1994.

- [14] H. C. Roters, *Electromagnetic Devices*. New York: Wiley; Chapman & Hall, 1941.
- [15] H. H. Woodson and J. R. Melcher, *Electromechanical Dynamics*. New York: Wiley, 1968.

Hector Martin Gutierrez was born in Lima, Peru, where he received the B.Sc. degree in applied mathematics from Universidad Cayetano Heredia, Lima, Peru, in 1989, and the B.Sc. degree in mechanical engineering from the Pontificia Universidad Catolica, Lima, in 1991. He received the M.Eng. degree in integrated manufacturing systems engineering in 1993, and the Ph.D. degree in electrical engineering in 1997, from North Carolina State University, Raleigh.

After working for two years as Lecturer for the Department of Mathematics and Physics, Universidad Cayetano Heredia, he joined North Carolina State University, working on nonlinear modeling and control of a long-range high-precision magnetically levitated fast-tool servo. He is currently a Postdoctoral Research Associate at the Center for Advanced Computing and Communications, North Carolina State University.

Paul I. Ro was born in Seoul, Korea, in 1959. He received the B.S. degree from the University of Minnesota, St. Paul, and the M.S. and Ph.D. degrees from the Massachusetts Institute of Technology, Cambridge, all in mechanical engineering in 1982, 1985, and 1989, respectively.

He became Assistant Professor in the Mechanical and Aerospace Engineering Department, North Carolina State University, Raleigh, in 1989, and was promoted to Associate Professor in 1994. In 1993, he was an ONR-sponsored Foreign Science Analyst at the University of Tokyo, Japan, studying precision actuators. In 1995, he was a Visiting Associate Professor at the Department of Machine Design and Production Engineering, Seoul National University, Korea. His fields of research are precision mechatronics and control, microdynamics of mechanical slides, ultra-high precision machining, magnetic servo levitation, nonholonomic motion planning and control, robotic assembly, and intelligent vehicle control.

He is a member of the ASME and ASPE (American Society of Precision Engineers), and is an Associate Editor of *Precision Engineering*, the journal of the ASPE.